Design, Synthesis, and Evaluation of Linear and Cyclic Peptide Ligands for PDZ10 of the Multi-PDZ Domain Protein MUPP1[†]

Sudhir C. Sharma,[‡] Chamila N. Rupasinghe,[‡] Rachel B. Parisien,[‡] and Mark R. Spaller*[,‡,§]

Department of Chemistry, Wayne State University, Detroit, Michigan 48202, and Department of Molecular Pharmacology, Brown University, Providence, Rhode Island 02912

Received April 29, 2007; Revised Manuscript Received August 16, 2007

ABSTRACT: PDZ10 is the 10th of 13 PDZ domains found within MUPP1, a cytoplasmic scaffolding protein first identified as an endogenous binding partner of serotonin receptor type 2c ($5HT_{2c}$). This association, as with those of several other interacting proteins that have subsequently been identified, is mediated through the C-terminal tail of the PDZ domain partner. Using isothermal titration calorimetry (ITC), we measured the thermodynamic binding parameters [changes in Gibbs free energy (ΔG), enthalpy (ΔH) and entropy ($T\Delta S$)] of the isolated PDZ10 domain for variable-length N-acetylated peptides from the $5HT_{2c}$ serotonin receptor C-terminal sequence, as well as for octapeptides of eight other putative partner proteins of PDZ10 ($5HT_{2a}$, hc-kit, hTapp1, mTapp2, TARP, NG2, claudin-1, and HPV-18 E6). In length dependence studies of the 5HT2c sequence, the maximal affinity of the peptides leveled off rapidly and further elongation did not significantly improve the dissociation constant (K_d) of 11 μM observed with the pentapeptide. Among the native partners of PDZ10, octapeptides derived from the hc-kit and $5HT_{2c}$ proteins were the strongest binders, with K_d values of 5.2 and 8.5 μM, respectively. The heat capacity change (ΔC_p) for the $5HT_{2c}$ octapeptide was determined to be −94 cal/mol, and a calculated estimate indicates burial of polar and apolar surface areas in equal measure upon ligand binding. Peptides with phosphoserine at either the P_{-1} or P_{-2} position experienced decreased affinity, which is in accord with the hypothesis that reversible phosphorylation is a possible mechanism for regulating PDZ domain-mediated interactions. Additionally, two conformationally constrained side chain-bridged cyclic peptide ligands were also designed, prepared, evaluated by ITC, and shown to bind PDZ10 primarily through a favorable change in entropy.

Even among the profusion of proteins that display a multiple-domain architecture, the multi-PDZ domain protein, or MUPP1,[1] is strikingly distinct. With 13 non-identical PDZ domains pearled from end to end, and absent of any apparent catalytic attributes, MUPP1 is enigmatic in its biological functions. First identified as a protein interacting with 5-hydroxytryptamine (5HT, serotonin) receptor type 2c ($5HT_{2c}$) in yeast two-hybrid screening (*1*, *2*), the corresponding mRNA transcripts were found to be abundant in the human brain and the peripheral organs, including heart, kidney, liver, testes, and skeletal muscle (*1*, *3*).

MUPP1 has been provisionally cast as a cytoplasmic scaffolding protein, serving, for example, within a signaling complex critical for synaptic NMDAR-dependent AMPA receptor trafficking in hippocampal neurons (*4*). These and a variety of other cellular indications serve as justification for the examination of portions of the MUPP1 substructure to illuminate the biochemical character of the different domains. In this study, focus is trained upon the 10th PDZ domain of MUPP1, PDZ10.

To elucidate the basic molecular recognition properties of PDZ10 and to establish a foundation for future cellular probe development for this particular domain and MUPP1 as a whole, two series of linear peptide ligands derived from the C-termini of endogenous protein partners have been prepared for binding evaluation. These comprise variable-length derivatives from $5HT_{2c}$ and fixed-length sequences from eight other assigned binding proteins. The analysis was conducted with isothermal titration calorimetry (ITC) such that detailed solution thermodynamic binding parameters would be obtained. Additionally, two bridged cyclic peptides, with corresponding linear control ligands, were likewise prepared and evaluated by ITC.

EXPERIMENTAL PROCEDURES

GST−PDZ10 Fusion Protein Expression and Purification. PDZ10 from rat MUPP1 was overexpressed as a soluble glutathione *S*-transferase (GST) fusion in *Escherichia coli* BL21-Gold (DE3) cells from a plasmid encoding GST−

[†] This research was supported by the National Institutes of Health (GM63021).

* To whom correspondence should be addressed. Phone: (401) 863-2946. Fax: (401) 863-1595. E-mail: mspaller@brown.edu.

[‡] Wayne State University.

[§] Brown University.

[1] Abbreviations: CD, circular dichroism; DTT, dithiothreitol; ESI-MS, electrospray ionization mass spectrometry; GST, glutathione *S*-transferase; HPV, human papillomavirus; ITC, isothermal titration calorimetry; MUPP1, multi-PDZ domain protein 1; NG2, membrane-spanning proteoglycan protein; PBS, phosphate-buffered saline; Tapp; tandem-pleckstrin-homology-domain-containing protein; TARP, transmembrane α-amino-3-hydroxyl-5-methyl-4-isoxazolepropionate (AMPA) receptor regulatory protein; 5HT, 5-hydroxytryptamine; PSD-95, postsynaptic density 95 protein.

10.1021/bi7008135 CCC: $37.00
Published on Web 10/16/2007

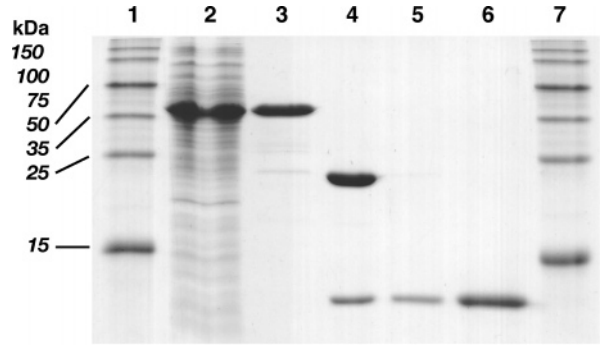

FIGURE 1: SDS−PAGE of MUPP1 PDZ10 expression and purification: lanes 1 and 7, molecular weight markers; lane 2, expressed bacterial lysate; lane 3, isolated GST−PDZ10 fusion protein after glutathione affinity column; lane 4, trypsin cleavage of the GST−PDZ10 fusion protein; lane 5, PDZ10 after glutathione affinity column; and lane 6, ion exchange purification of PDZ10.

PDZ10 within a pGEX-2T vector (provided by R. Andrade, Wayne State University). The construct was subcloned such that the thrombin recognition and downstream MUPP1 sequence encoded LVPRGSPEFMKDSSQT. A single colony of the cells transformed with the GST−PDZ10 plasmid was cultured in LB medium (10 mL) with 50 μg/mL ampicillin at 37 °C for 12 h. The cells were diluted 1:200 (5 mL of culture into 995 mL of fresh medium) and were grown at 37 °C until an OD_{600} of ~1.2 was reached. The culture was then induced with 0.8 mM isopropyl β-D-thiogalactoside (IPTG) at 30 °C for 6 h to overexpress the fusion protein. The cells were harvested by centrifugation at 3220*g* for 20 min at 4 °C. The cells were resuspended in 1× PBS [10 mM phosphate, 137 mM NaCl, and 2.7 mM KCl (pH 7.4)] containing 1% Triton-X and 19 mM β-mercaptoethanol. The cells were sonicated (Branson sonifier; 55 s, duty cycle of 50%, output control of 5), and the lysate was centrifuged at 10000*g* for 20 min at 4 °C to remove insoluble cellular debris. The supernatant was applied to a GST affinity column prepared from glutathione−agarose beads (5 mL; Sigma). The column was washed and equilibrated with 15 volumes of 1× PBS and eluted with 3−4 column volumes of 50 mM Tris-HCl (pH 8.0) containing 5 mM reduced glutathione.

MUPP1 PDZ10 Isolation and Purification. To remove the N-terminal GST, the GST−PDZ10 fusion protein was proteolytically cleaved using TPCK trypsin (Pierce) at a 1:700 ratio (trypsin:GST−PDZ10, w/w) at room temperature for 2 h, dialyzed in 1× PBS with 1 mM DTT at 4 °C, and then loaded onto a glutathione−agarose column. After affinity purification, the sample was dialyzed into sodium phosphate (10 mM, pH 6.0) containing DTT (1 mM) and then further purified by Q HP Sepharose (Pharmacia) ion exchange chromatography using a sodium chloride gradient (from 20 to 80 mM NaCl in 10 steps) in sodium phosphate (10 mM, pH 6.0) with DTT (1 mM). The elution fraction containing PDZ10 (usually 50−65 mM NaCl) was pooled, dialyzed in sodium phosphate (10 mM, pH 7.0) with DTT (1 mM) at 4 °C, and concentrated using a centrifugal filter device (Millipore, 5000 MWCO). The concentration of the purified PDZ10 was estimated with the Advanced Protein Assay (Cytoskeleton). An SDS−PAGE depicting every state of isolation and purification confirmed the expected size and purity of each protein isolate (Figure 1).

PDZ10 Characterization. In addition to DNA sequencing confirming the identity of the residues encoded by the expression vector, the purified PDZ10 sample was subjected to N-terminal protein sequencing (Macromolecular Structure Facility, Michigan State University, East Lansing, MI) and ESI mass spectrometric analysis. The PDZ10 solution conformation was examined by CD spectroscopy (OLIS-CD spectropolarimeter) in a solution of sodium phosphate (20 mM), NaCl (100 mM), and DTT (1 mM) at pH 7.0. CD spectra were recorded over a range of 190−260 nm at 4, 15, 25, and 40 °C, in a Helma quartz cell (1 mm path length and a volume of 300 μL) with CD spectra of the buffer as a baseline reference.

Unmodified Linear Peptide Preparation. The sequences selected for synthesis matched the C-terminal regions of the protein partners; these were hc-kit (*5*) (NP_000213), $5HT_{2c}$ (*2*) (NP_000859), $5HT_{2a}$ (*2*) (NP_000612), mTapp2 (*6*) (NP_112547), hTapp1 (*6*) (NP_067635), TARP (*7*) (NP_055220), NG2 (*8*) (NP_112284), claudin-1 (*9*, *10*) (NP_066924), and HPV-18 E6 (*11*) (NP_040310). Linear peptides were manually prepared and purified using standard Fmoc-based solid-phase synthesis protocols in a manner commensurate with our earlier published procedures (*12*).

All syntheses utilized preloaded Val-NovaSyn TGA resin (0.125 mmol of Val loading, 250 mg of resin) loaded into a peptide synthesis reaction vessel mounted on a wrist-action shaker. The initial suspension and swelling of the resin (45 min) took place with shaking using dichloromethane (DCM) followed by washing. Thereafter, the procedure consisted of iterative deprotection and coupling steps with interspersed washing steps. Fmoc deprotection was effected with piperidine-DMF (20%, v/v; 10 × the resin volume) for 10 min, washing, and a repeat with fresh deprotection solvents for 10 min, followed by DMF washing (10 × the resin volume). Sequential coupling of residues involved mixing of Fmoc-amino acid (0.375 mmol), DIPCI (0.500 mmol), HOBt (0.750 mmol), HBTU (0.375 mmol), and DMF (5 × the resin volume) with gentle shaking for 2 h.

The Kaiser test was used to confirm complete coupling, as indicated by a negative result; if the coupling was incomplete, additional DIPCI (0.125 mmol) was added and the vessel shaken for an additional 2 h. If the coupling was complete, the solution was drawn off and the resin was washed with DMF (10 × the resin volume). Coupling and deprotection steps were repeated for each added residue, with intervening washing steps (DMF, 10 × the resin volume).

After the final Fmoc deprotection and sequential DCM and DMF washing, N-terminal acetylation was effected by adding 3 mL of an acetic anhydride/pyridine/DMF (1:1:8, v/v) solution to the resin in the vessel. After 30 min with gentle shaking, the resin was sequentially washed with DCM, DMF, ethyl ether, and acetone (twice each, 10 × the resin volume). Finally, the resin cleavage solution [5 × the resin volume, TFA/TIS (triisopropylsilane)/thioanisole/anisole, 92:4:2:2, v/v] was added with shaking for 2 h. The solution was collected and separated equally into two 10 mL test tubes, followed by addition of ethyl ether (−20 °C) to reach 80% of the total tube capacity. The solution was mixed, and the peptide precipitate formed immediately. After centrifugation (8 min at 6000 rpm), the supernatant was decanted, fresh ether was added, and the pelleted peptide was mixed before another round of centrifugation (repeated three additional times). Finally, the peptide was dissolved in distilled water

(5−10 mL), frozen, and lyophilized for 24−48 h until a white powder was obtained. Peptides were purified by RP-HPLC, and molecular masses were confirmed by ESI and MALDI-TOF mass spectroscopy.

Phosphorylated Linear Peptide Preparation. The same synthetic route was followed that was used for the unmodified linear peptides, but adapted for the incorporation of Fmoc-Ser(PO(OBzl)OH)-OH (0.375 mmol) using the following coupling conditions: DIPCI (0.500 mmol), HOBt (0.250 mmol), HBTU (0.375 mmol), TBTU (0.375 mmol), and DMF (5 × the resin volume) with gentle shaking for 2 h.

Linear Control Peptide Preparation. Compounds **Linear-1**, **Linear-2a**, and **Linear-2b** were prepared and purified in the manner described above for the unmodified peptides (starting with 0.125 mmol of resin), except that N_ϵ-acetyl-L-lysine was used at the appropriate position in the synthetic scheme. For compound **Linear-2b**, an additional modification was required [Fmoc-Glu(*O*-2-PhiPr)-OH was used]. After synthesis of the entire linear peptide in the standard fashion (but before final Fmoc deprotection and resin cleavage), the Glu side chain was removed using a TFA/EDT/DCM solution (2:5:93, v/v; 10 × the resin volume) added three times for 30 min each time. Methylamine [2 M in THF (Acros); 3.0 mmol], DIPCI (4.0 mmol), and HOBt (6.0 mmol) were added to form the amide with the deprotected carboxylic acid side chain of Glu. The previously described methods were then used to acetylate, cleave, purify, and characterize the peptides.

Cyclic Peptide Preparation. Beginning as before with Val-NovaSyn TGA resin (0.125 mmol), standard steps were used to elongate the peptide to four residues, in the following order: Fmoc-Val-Wang resin, Fmoc-Glu(O-2-PhiPr)-OH, Fmoc-Ser(tBu)-OH, and Dde-Lys(Fmoc)-OH. Removal of the Lys side chain Fmoc with a standard piperidine-DMF solution was followed by DIPCI-mediated coupling to the exposed carboxylate of Fmoc-β-Ala. The *O*-2-PhiPr protecting group of Glu was removed with the TFA/EDT/DCM solution (2:5:93, v/v; 10 × the resin volume) added three times for 30 min each time. Piperidine-DMF was used to deprotect the Fmoc on the now-coupled β-Ala. The resin was washed with 10% DIPEA in DCM (v/v, 10 × the resin volume) three times for 3 min each time to disrupt potential salt bridge formation. Following this, the resin was once again washed with DMF (10 times with 10 × the resin volume). DMSO (25%) in NMP (v/v, 10 × the resin volume) was added to the reaction vessel to prevent aggregation of the resin.

The coupling of the β-Ala amine with the Glu side chain carboxylate to close the macrocycle was effected by the addition of BOP (3.0 mmol), DIPEA (6.0 mmol), and HOBt (3.0 mmol); the vessel was left to shake for 2 h. The resin was washed with DMF (10 times, 10 × the resin volume) and DCM (5 times, 10 × the resin volume), followed by removal of the N-terminal Dde protecting group Lys using 2% hydrazine in DMF (v/v, 10 × the resin volume). The duration of the hydrazine/DMF exposure was 10 min, followed by draining and repetition of these deprotection conditions three more times. The resin was once again washed with DMF (10 times with 10 × the resin volume). At this point, standard peptide synthesis and characterization procedures as described for the unmodified linear peptides were followed to complete the ligand synthesis and purification.

Isothermal Titration Calorimetry. Calorimetry experiments were performed with a VP-ITC microcalorimeter (Microcal Inc.). Typical experiments involved direct injections of peptide ligands into the sample cell containing PDZ10. Prior to each titration, PDZ10 samples were extensively dialyzed in sodium phosphate (10 mM, pH 7.0) with DTT (1 mM). Peptides were dissolved in the actual buffer that was last used to dialyze the protein sample. The pH of the peptide was adjusted to match (within ±0.02 pH unit) that of the PDZ10 sample by titrating with ca. 1−2 μL of either 4 M NaOH or HCl solution in submicroliter aliquots (total volume of the peptide solution being ∼1.5 mL). Typical concentrations of PDZ10 used ranged from 70 to 150 μM, and those of the peptides ranged from 1 to 2 mM. Titration experiments were designed so that the *c* values (*13*) were greater than 1, ranging between 2 and 38 [with the exception of those of the low-affinity peptides Ac-QRRRETQV (HPV-18 E6), Ac-VSERIS(PO$_4$)SV, and Ac-VSERISS(PO$_4$)V, where this cannot be maintained due a requirement for a very high protein concentration]. Both PDZ10 and peptide samples were degassed for 20 min in a thermovac without stirring. Experiments were conducted at a reference power of 10 μcal/s, a stirring speed of 270 rpm, and a sample cell temperature of 25 °C.

For the aforementioned low-affinity peptides whose titrations into protein sample were marked by small *c* values ($c < 1$), competitive experiments were performed by titrating known high-affinity ligands into a protein solution also containing a saturating concentration of the weaker-binding peptide (the affinity of which is to be determined), according to an established procedure (*14*). In brief, a protein sample of 85−110 μM was presaturated with ca. 0.9−1.0 mM (i.e., 10-fold molar excess) of the lower-affinity peptide before titration with ca. 1.1 mM high-affinity peptide (either Ac-VSLRTSDV or Ac-VSLRVSSV) in the presence of ca. 0.9−1.0 mM low-affinity peptide. This formulation addresses the requirement that the concentration of the lower-affinity peptide be the same in the protein solution as well as in that of the high-affinity peptide solutions, to prevent buffer mismatch. All other experimental conditions were the same as described earlier for the standard calorimetric titrations. For these ligands, the *c* values are "apparent" values for the titration of the high-affinity peptide into protein presaturated with low-affinity peptide.

For the determinations of the change in heat capacity (ΔC_p), separate experiments were performed at 15, 25, and 35 °C, in the same manner as described earlier for the standard calorimetric titrations. For experiments in which the buffer heat of ionization (ΔH_{ion}) was varied, separate titrations were carried out in 10 mM sodium phosphate, 10 mM Tris-HCl (with 10 mM NaCl), and 10 mM Hepes (with 10 mM NaCl). Each buffer was prepared at pH 7.0. Origin (version 5) was used to process the data with the one-binding site model.

Heats of dilution of the peptide were initially measured as "blank titrations" by injecting the peptide solution into the buffer placed in the ITC sample cell and subtracted from the observed "raw heat" values. It was determined that these values were comparable to those obtained from the last few injections at the end of the actual peptide-into-protein

FIGURE 2: Comparison of trypsin and predicted thrombin cleavage of PDZ10 sequences. The predicted thrombin-processed PDZ10 polypeptide comprises 141 residues (top sequence), while trypsin actually cuts at internal sites on both the C- and N-terminal sides, resulting in a polypeptide of 109 residues (bottom sequence).

titration, after saturation (except for the few cases involving low-affinity peptides). Subsequently, subtraction of the heat values of the tail end dilution peaks was used for the correction of the raw data for the reported ITC experiments. The control experiments involving titration of buffer into buffer, and buffer into PDZ10 sample, afforded insignificant heats of dilution.

RESULTS

Preparation and Characterization of PDZ10. Primary requisites for an extended ITC study are the availability of the protein component in relatively large quantities (i.e., milligram scale) and confirmation that the form obtained maintains structural integrity over the range of temperatures to be employed. Using the expression vector pGEX-2T, the GST−PDZ10 fusion was expressed in *E. coli* BL21-Gold (DE3) cells on the order of ca. 160 mg/L of culture. The fusion protein was proteolytically cleaved with trypsin and affinity purified to remove GST. The resulting PDZ10 was further purified by ion exchange chromatography with a typical yield of 30 mg/L of culture. Each step of the protein purification procedure was visually documented by SDS−PAGE analysis, culminating in a single sharp band for isolated PDZ10 (Figure 1).

The result of N-terminal protein sequencing of the trypsin-derived PDZ10 sample revealed an amino terminus of SSTP. When mapped against the amino acid sequence of the PDZ10 construct as determined by DNA sequencing of the PDZ expression vector, this would result from cleavage at the C-terminus of arginine, which is 28 residues inside the N-terminal region of the predicted thrombin-cleaved polypeptide product. ESI mass spectroscopy determined the mass of the PDZ10 sample to be 11 643 Da. Taken together, these two pieces of data correlate with a 109-residue PDZ10 polypeptide that begins with SSTP and ends with the sequence LYRDEAPR (Figure 2). The MUPP1 sequence used corresponds to that of RefSeq accession NP_062069, except that the sixth residue in our construct is V instead of I and the last residue (R) is from the subcloning construct as the 3′ stop codon is downstream of R, after four residues. The purified PDZ10 protein was subjected to CD spectral analysis at 4, 25, and 40 °C. The result of monitoring the ellipticity signal versus the wavelength indicates that the overall folding pattern for PDZ10 remains nearly the same at each of the temperatures that were tested (see the Supporting Information). The spectra did not show any significant change at the wavelengths of primary concern (200−240 nm).

Effect of Buffer and Determination of Protonation Events. Since events besides the actual binding interaction can contribute to the observed enthalpy change, it is necessary to identify such interference. The measured, apparent, or observed change in enthalpy (here reported as ΔH) from calorimetry is the sum of the change in the heat of enthalpy of intrinsic ligand binding (ΔH_{bind}) and a product involving the change in enthalpy of ionization (ΔH_{ion}) of the employed buffer, as shown by eq 1, which can be calculated by performing experiments at different buffers with known ΔH_{ion} values.

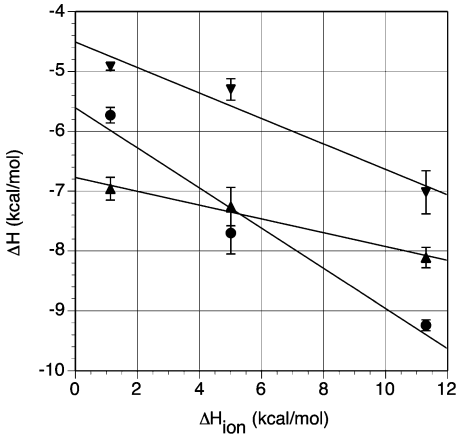

FIGURE 3: Determination of proton exchange upon binding for selected PDZ10 peptides. Values (in proton equivalents) determined from slopes are as follows: Ac-VNEKVSCV (▼), −0.21; Ac-VSLRVSSV (●), −0.34; and Ac-VSERISSV (▲), −0.12.

$$\Delta H = \Delta H_{bind} + (n_{H^+})\Delta H_{ion} \quad (1)$$

The variable n_{H^+} is the number of protons exchanged with buffer upon complex formation. The ΔH values of PDZ10 with the $5HT_{2c}$, $5HT_{2a}$, and Ac-VSLRVSSV peptides at 25 °C in three different buffers (phosphate, HEPES, and Tris) with different heats of ionizations, ΔH_{ion}, are plotted in Figure 3. As the ΔH_{ion} values of the buffers increase, ΔH values decrease, indicating the release of proton equivalents into the buffer medium (see the Supporting Information). Here the number of protons involved for $5HT_{2c}$, $5HT_{2a}$, and Ac-VSLRVSSV were −0.12 ± 0.02, −0.21 ± 0.05, and −0.34 ± 0.07 per mole, respectively.

Thermodynamics of Binding for PDZ10 with $5HT_{2c}$ Peptides. The first stage of this study entailed measurement of binding properties as a function of ligand length. Seven N-acetylated peptides comprising 4−10 residues of the C-terminal region of the $5HT_{2c}$ receptor were prepared, and their thermodynamic parameters with PDZ10 were measured by ITC (Table 1 and Figures 4 and 5). K_d values ranged from 57 to 8.5 μM. The seven-residue peptide exhibited the lowest contribution from ΔH and highest contribution from

Table 1: Thermodynamic Parameters for Binding of Variable-Length $5HT_{2c}$ Peptide Ligands to MUPP1 PDZ10[a]

peptide	K_d (μM)	ΔG (kcal/mol)	ΔH (kcal/mol)	$T\Delta S$ (kcal/mol)	n[b]	c[c]
Ac-ISSV	57 (1)	−5.8 (0.1)	−5.3 (0.1)	0.5 (0.1)	0.80 (0.01)	3
Ac-RISSV	11 (1)	−6.7 (0.1)	−6.1 (0.1)	0.6 (0.1)	1.07 (0.01)	11
Ac-ERISSV	9.8 (0.6)	−6.8 (0.1)	−5.9 (0.1)	0.9 (0.1)	1.08 (0.01)	13
Ac-SERISSV	12 (1)	−6.7 (0.1)	−5.2 (0.1)	1.5 (0.1)	1.15 (0.04)	8
Ac-VSERISSV	8.5 (0.4)	−6.9 (0.1)	−7.0 (0.2)	−0.1 (0.2)	1.01 (0.05)	17
Ac-VVSERISSV	11 (2)	−6.8 (0.1)	−6.4 (0.2)	0.4 (0.1)	0.94 (0.02)	10
Ac-NVVSERISSV	10 (1)	−6.8 (0.1)	−6.6 (0.1)	0.2 (0.1)	0.92 (0.08)	13
Ac-VSERITSV	13 (1)	−6.7 (0.1)	−5.5 (0.2)	1.2 (0.1)	1.01 (0.04)	10
ERISSV[d]	4.8 (0.7)	−7.3 (0.1)	−6.2 (0.4)	1.1 (0.5)	1.05 (0.02)	26
NVVSERISSV[d]	2.6 (0.1)	−7.6 (0.1)	−5.5 (0.1)	2.1 (0.1)	1.15 (0.05)	38

[a] Values are the means of at least two independent titrations, with errors given in parentheses. [b] Binding stoichiometry (peptide:protein). [c] $c = (K_a)$(concentration of binding site). [d] Peptides bearing a free amino terminus.

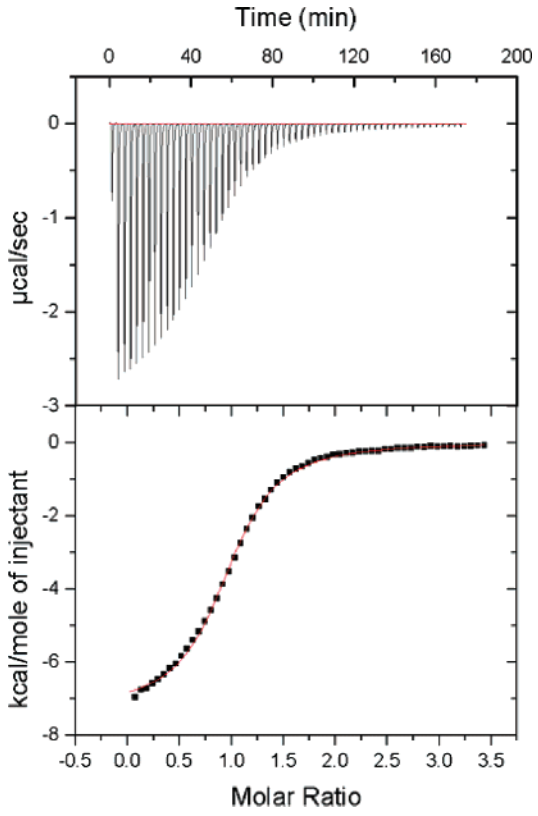

FIGURE 4: ITC data for titration of the $5HT_{2c}$ octapeptide (Ac-VSERISSV) into MUPP1 PDZ10 in phosphate buffer. The top panel shows the titration thermogram; the bottom panel shows the best curve fit for the integrated data.

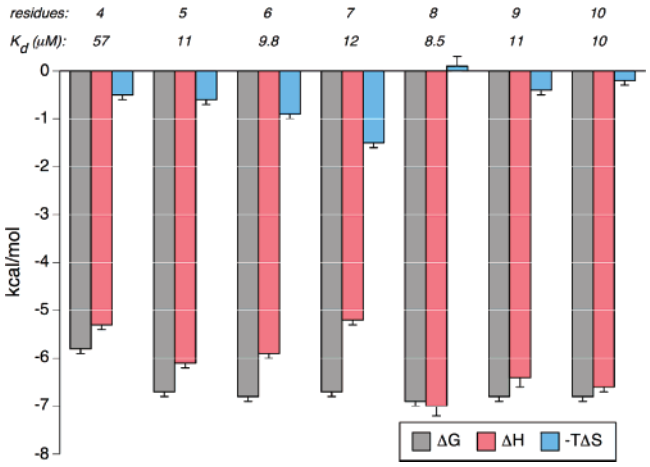

FIGURE 5: Thermodynamic binding parameters for PDZ10 and variable-length $5HT_{2c}$ peptide ligands. Note that $T\Delta S$ values are depicted as their negative values for graphical convenience.

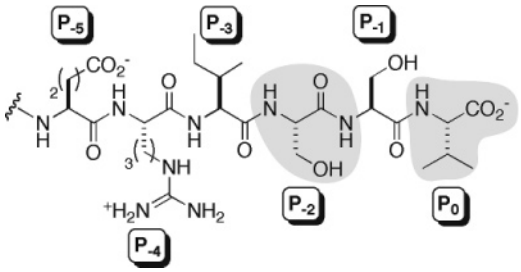

FIGURE 6: Labeling convention for the PDZ domain-binding motif for the C-terminus of the $5HT_{2c}$ peptides. Shaded are the two positions, P_0 and P_{-2}, considered most pivotal for binding affinity in the majority of PDZ domains characterized to date.

$T\Delta S$, while the reverse is the case when one Val residue is added to yield the octapeptide. For the series, then, that single residue transition represents the largest $\Delta\Delta H$ at −1.8 kcal/mol. A corresponding affinity enhancement is not observed, however, due to a closely matched compensation by entropy. The transition from tetra- to pentapeptide, representing the largest jump in affinity of the series, is driven by a modest improvement in the enthalpy ($\Delta\Delta H$) of −0.8 kcal/mol.

To gauge the effect of the free amino group at the N-terminus, we prepared two peptides based on the $5HT_{2c}$ sequence, with free (non-acetylated) amino termini, with lengths of 6 and 10 residues. Binding analysis with PDZ10 revealed a 2- and 3-fold increase in binding affinity, respectively, over the corresponding N-acetylated versions.

As class I PDZ domains are defined in part as requiring either serine or threonine at the critical P_{-2} position of their ligands, to establish the residue preference for PDZ10 a mutant $5HT_{2c}$ octapeptide with Thr in place of Ser at position P_{-2} (Figure 6) was tested. This analogue, Ac-VSERITSV, was slightly less favored over the parent peptide with native Ser (Table 1). We then examined whether the protein can tolerate the third standard amino acid bearing a hydroxyl side chain, Tyr, at that critical position. Given the spatially different positioning, this was considered unlikely, and unsurprisingly, the analogue with Tyr at P_{-2} showed no detectable binding for PDZ10 (i.e., no heat signals above dilution were recorded).

Thermodynamics of Binding for PDZ10 with the Phosphorylated Peptide. The effect of the presence or absence of phosphate on peptide ligands for PDZ10 was examined due to the ramifications that this might have on the

Table 2: Thermodynamic Parameters for Binding of Phosphorylated $5HT_{2c}$ Peptides to MUPP1 PDZ10[a]

peptide	K_d (μM)	ΔG (kcal/mol)	ΔH (kcal/mol)	$T\Delta S$ (kcal/mol)	n[b]	c[c]
Ac-VSERISSV	8.5 (0.4)	−6.9 (0.1)	−7.0 (0.2)	−0.1 (0.2)	1.01 (0.05)	17
Ac-VSERIS(PO$_4$)SV[d]	323 (24)	−4.8 (0.1)	−5.8 (0.4)	−1.0 (0.4)	0.89 (0.05)	4
Ac-VSERIS̲S̲(PO$_4$)V[d]	237 (64)	−5.0 (0.2)	−5.4 (0.2)	−0.4 (0.1)	0.86 (0.06)	4

[a] Values are the means of at least two independent titrations, with errors given in parentheses. [b] Binding stoichiometry (peptide:protein). [c] $c = (K_a)$(concentration of binding sites). [d] Phosphorylated serine indicated by the underlined position. Values obtained by competitive titration of Ac-VSLRTSDV into PDZ10 saturated with phosphorylated peptide. n and apparent c values reported here are for the titration of Ac-VSLRTSDV into PDZ10 presaturated with the phosphorylated peptide.

Table 3: Thermodynamic Parameters for Binding of Protein Partner-Derived Peptide Ligands to MUPP1 PDZ10[a]

	peptide	K_d (μM)	ΔG (kcal/mol)	ΔH (kcal/mol)	$T\Delta S$ (kcal/mol)	n[b]	c[c]
hc-kit	Ac-PLLVHDDV	5.2 (0.1)	−7.2 (0.1)	−10.5 (0.4)	−3.3 (0.4)	0.85 (0.01)	16
$5HT_{2c}$	Ac-VSERISSV	8.5 (0.4)	−6.9 (0.1)	−7.0 (0.2)	−0.1 (0.2)	1.01 (0.05)	17
$5HT_{2a}$	Ac-VNEKVSCV	17 (1)	−6.5 (0.1)	−4.9 (0.1)	1.6 (0.1)	0.94 (0.05)	8
mTapp2	Ac-ENIRTSDV	22 (1)	−6.4 (0.1)	−6.2 (0.1)	0.2 (0.1)	0.99 (0.07)	4
hTapp1	Ac-ASLPVSDV	24 (1)	−6.3 (0.1)	−4.4 (0.2)	1.9 (0.2)	0.99 (0.13)	7
TARP	Ac-LNRRTTPV	33 (1)	−6.1 (0.1)	−2.5 (0.2)	3.6 (0.2)	0.97 (0.10)	4
NG2	Ac-LRNGQYWV	37 (1)	−6.0 (0.1)	−1.0 (0.1)	5.0 (0.1)	0.87 (0.03)	3
claudin-1	Ac-PSSGKDYV	77 (5)	−5.6 (0.1)	−3.0 (0.1)	2.6 (0.1)	1.08 (0.03)	2
E6[d]	Ac-QRRRETQV	221 (24)	−5.0 (0.1)	−4.9 (0.1)	0.1 (0.2)	0.87 (0.04)	5

[a] Values are the means of at least two independent titrations, except for the E6 peptide, with errors given in parentheses. [b] Binding stoichiometry (peptide:protein). [c] $c = (K_a)$(concentration of binding sites). [d] Values obtained by competitive titration of Ac-VSLRVSSV into PDZ10 presaturated with Ac-QRRRETQV. n and apparent c values reported here for Ac-QRRRETQV were obtained for the titration of Ac-VSLRVSSV into PDZ10 presaturated with Ac-QRRRETQV.

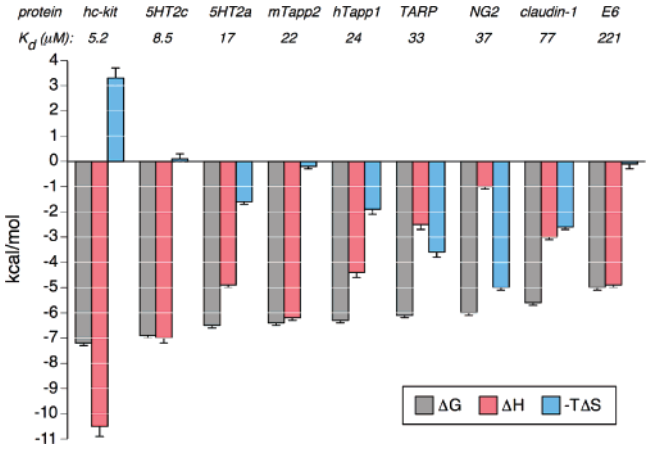

FIGURE 7: Thermodynamic binding parameters for PDZ10 and octapeptide ligands derived from protein partners. Note that $T\Delta S$ values are depicted as their negative values for graphical convenience.

corresponding activity in cells. To evaluate the binding consequences of phosphorylation of Ser upon binding affinity, Ser residues at P_{-2} and P_{-1} in $5HT_{2c}$ peptides were separately changed to phosphoserines. Thus, two separate peptides, one with phosphoserine at P_{-1} and another at P_{-2}, were prepared, and their binding attributes with respect to PDZ10 were evaluated (Table 2). When compared to the unmodified $5HT_{2c}$ peptide, the peptide with the phosphoserine substitution at P_{-2} had an almost 40-fold lower affinity, while phosphoserine at P_{-1} reduced binding strength 30-fold.

Thermodynamics of Binding for PDZ10 with Partner Protein Peptides. After the analysis of the $5HT_{2c}$ peptides, the second stage examined the thermodynamic binding parameters as a function of diverse sequence composition, as embodied in known partner proteins of MUPP1 PDZ10. Among the natural binders of this domain, the hc-kit peptide exhibited the highest affinity, with a K_d value of 5.2 μM (Table 3 and Figure 7). $5HT_{2c}$ peptide is the next highest-affinity peptide ($K_d = 8.5$ μM), with favorable enthalpy and nearly noncontributing entropy. The hTapp1 and mTapp2 peptides have comparable affinities, with binding constants of 24 and 22 μM, respectively. Peptides derived from NG2 and TARP proteins also have similar affinities. The claudin-1 peptide has a modest affinity ($K_d = 77$ μM), and the HPV-18 E6 protein yielded the weakest peptide for PDZ10 ($K_d = 245$ μM).

Toward an Optimized Consensus Sequence. While an accurate assessment of binding parameters of ligands recapitulating native interactions contributes to our basic understanding of the endogenous interaction, modifications to improve ligand affinity are desirable for the purpose of generating cellular probes for later in vivo experiments. After examination of the sequences of PDZ10 binders and their dissociation constants, an effort was made to identify specific residues at the P_{-1}, P_{-3}, and P_{-5} positions that might be important for strong association. Substitution of Leu (as in hc-kit and hTapp1 peptides) at P_{-5} and Thr (as in mTapp2 and TARP peptides) at P_{-3} in the corresponding N-acetylated $5HT_{2c}$ octapeptide led to the original consensus peptide Ac-VSLRTSSV, which shows a slight improvement in the affinity over that of $5HT_{2c}$ peptide (Table 4). A replacement with Asp (as in the hc-kit, hTapp1, and mTapp2 peptides) at the P_{-1} position of the original consensus sequence yielded no significant change in affinity. Further substitution with Val (as in the $5HT_{2a}$ and hTapp1 peptides) at P_{-3} afforded a ligand with substantially larger enthalpic contributions; as a consequence of the opposing entropic change, however, the affinity remained essentially unaffected. When only Thr at P_{-3} of the original consensus peptide is replaced with Val, the resulting Ac-VSLRVSSV peptide possesses a slightly improved binding affinity ($K_d = 4.2$ μM).

Change in Heat Capacity (ΔC_p). Beyond the primary values of ΔG, ΔH, and ΔS, the change in heat capacity is a

Table 4: Thermodynamic Parameters for Binding of Consensus Peptides to MUPP1 PDZ10[a]

peptide	K_d (μM)	ΔG (kcal/mol)	ΔH (kcal/mol)	$T\Delta S$ (kcal/mol)	n[b]	c[c]
Ac-VSLRTSSV	5.5 (0.1)	−7.2 (0.1)	−6.2 (0.1)	1.0 (0.1)	0.84 (0.03)	23
Ac-VSLRTSDV[d]	6.2 (0.1)	−7.1 (0.1)	−7.7 (0.2)	−0.6 (0.2)	0.90 (0.01)	20
Ac-VSLRVSDV[d]	5.4 (0.2)	−7.2 (0.1)	−8.6 (0.1)	−1.4 (0.1)	0.91 (0.01)	18
Ac-VSLRVSSV[d]	4.2 (0.1)	−7.3 (0.1)	−5.7 (0.1)	1.6 (0.1)	0.96 (0.03)	31

[a] Values are the means of at least two independent titrations, with errors given in parentheses. [b] Binding stoichiometry (peptide:protein). [c] $c = (K_a)$(concentration of binding sites). [d] Underlined residues denote residues that differ from the original consensus peptide, Ac-VSLRTSSV.

Table 5: Changes in Heat Capacity and Estimations of Polar and Apolar Surface Areas

peptide	ΔC_p (cal mol^{-1} K^{-1})	ΔASA_{polar} (Å^2)	ΔASA_{apolar} (Å^2)
$5HT_{2c}$ (Ac-VSERISSV)	−94 (7)	−452 (15)	−469 (24)
$5HT_{2a}$ (Ac-VNEKVSCV)	−100 (1)	−387 (2)	−445 (3)
$5HT_{2a}$ (Ac-VSLRVSSV)	−140 (7)	−499 (13)	−598 (23)

desirable parameter to determine in the course of a protein−ligand interaction. ΔC_p offers a measure of the perturbation of hydration of a biomolecular system (*15*, *16*) and, as such, provides information about the degree of solvent exchange that occurs during a binding event. ΔC_p is determined from the temperature dependence of the ΔH as defined by eq 2.

$$\Delta C_p = \frac{d\Delta H}{dT} \quad (2)$$

Calorimetric experiments were performed in phosphate buffers for three representative ligands, high-affinity peptide Ac-VSLRVSSV and native peptides $5HT_{2c}$ and $5HT_{2a}$, at 10 °C intervals from 15 to 35 °C in phosphate buffer at pH 7.0. The resulting ΔH values for these associations change linearly with temperature, whereas those of ΔG remain nearly constant (see the Supporting Information). The linearity of the change in enthalpy as a function of temperature provides a measure of support for the fact that the thermodynamic parameters obtained are direct consequences of the binding event in question, and absent of any other coupled equilibria occurring upon complex formation (*17*). The ΔC_p values obtained for the $5HT_{2c}$, $5HT_{2a}$, and Ac-VSLRVSSV peptides

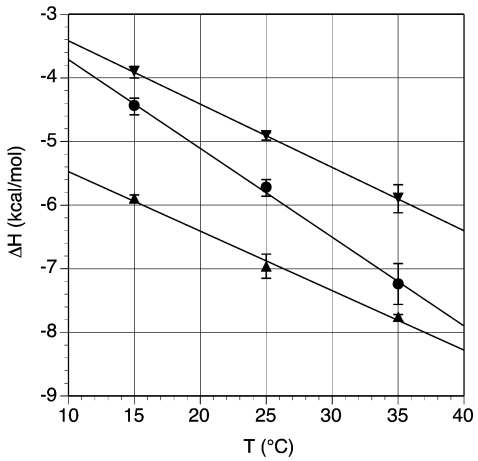

FIGURE 8: Determination of changes in heat capacity (ΔC_p) upon binding for selected PDZ10 peptides. Values (in calories per mole per kelvin) determined from slopes are as follows: Ac-VNEKVSCV (▼), −100; Ac-VSLRVSSV (●), −140; and Ac-VSERISSV (▲), −94.

were −94, −100, and −140 cal mol^{-1} K^{-1}, respectively (Table 5 and Figure 8). A negative sign for ΔC_p is a distinctive feature of site-specific binding, and the modest magnitude of ΔC_p is suggestive of rigid body interactions without significant conformational changes in the protein (*18*). Comparable results for ΔC_p have been reported for SHC domain (*19*), SH2 domain (*20*, *21*), and chaperone SecB substrate binding (*22*). The ΔC_p values were also used to estimate burial of solvent accessible polar and apolar surface areas (see the Discussion).

Cyclic Peptide Ligands for PDZ10. While linear peptides often serve as cellular probes, constrained peptides—such as those that are cyclic—can prove to be more desirable, particularly in terms of biological stability. With this objective, we applied our "bridged cyclic" design for PDZ domain macrocycles (*23*) to the PDZ10 ligand framework. Without structural information to guide the choice of constraining elements to join the side chains of the P_{-1} glutamate and P_{-3} lysine, a β-alanine linker was used. This particular bridging unit had proven successful in our previous ligand design effort targeting the third PDZ domain (PDZ3) of PSD-95 (*23*). On the basis of the C-terminal sequence of $5HT_{2c}$, a cyclic peptide (**Cyclic-1**; RP1007) and an approximate linear control (**Linear-1**; RP1001) were prepared and calorimetrically tested as ligands for PDZ10 (Figure 9 and Table 6). **Cyclic-1** has an affinity of 30 μM due primarily to a favorable entropic contribution, with a $T\Delta S$ of 3.4 kcal/mol (Table 6). The linear peptide as a control with glutamine at P_{-1} and N_ϵ-acetyl-L-lysine at P_{-3} gave similar K_d values, exhibiting a primarily enthalpic interaction.

A second cyclic peptide (**Cyclic-2**; RP1115) was prepared on the basis of the high-affinity peptide Ac-VSLRVSSV. Two linear control peptides were also synthesized, one with glutamine at P_{-1} and N_ϵ-acetyl-L-lysine at P_{-3} (**Linear-2a**; RP1077), the other bearing a P_{-1} N-methylated glutamine side chain and N_ϵ-acetyl-L-lysine at P_{-3} (**Linear-2b**; RP1113). **Cyclic-2** bound PDZ10 3-fold better than **Cyclic-1**, with a K_d of 11 μM. **Cyclic-2** had a slightly elevated $T\Delta S$ contribution compared to those of the linear controls, 4.6 kcal/mol as opposed to 3.8 kcal/mol (**Linear-2a**) and 3.5 kcal/mol (**Linear-2b**). However, the cyclization failed to improve the affinity as both linear control peptides retained K_d values on the order of 10 μM.

DISCUSSION

MUPP1 Engages in Varied Activities. PDZ domain-mediated interactions are increasingly recognized as a major mode through which cellular networks effect protein−protein interactions (*24*, *25*). MUPP1, with its baker's dozen of PDZ domains, is implicated in a number of biochemically diverse cellular processes. One of several documented roles is that

Table 6: Thermodynamic Parameters for Binding of Bridged Cyclic and Linear Control Peptide Ligands to MUPP1 PDZ10[a]

peptide	K_d (μM)	ΔG (kcal/mol)	ΔH (kcal/mol)	$T\Delta S$ (kcal/mol)	n[b]	c[c]
Cyclic-1 (RP1007)	30 (1)	−6.2 (0.1)	−2.8 (0.1)	3.4 (0.1)	1.04 (0.03)	4
Linear-1 (RP1001)	31 (1)	−6.1 (0.1)	−5.0 (0.1)	1.1 (0.1)	0.85 (0.01)	5
Cyclic-2 (RP1115)	11 (1)	−6.8 (0.1)	−2.2 (0.1)	4.6 (0.1)	0.84 (0.02)	8
Linear-2a (RP1077)	11 (1)	−6.8 (0.1)	−3.0 (0.1)	3.8 (0.1)	0.99 (0.09)	9
Linear-2b (RP1113)	10 (1)	−6.8 (0.1)	−3.3 (0.1)	3.5 (0.1)	0.84 (0.01)	9

[a] Values are the means of at least two independent titrations, with errors given in parentheses. [b] Binding stoichiometry (peptide:protein). [c] c = (K_a)(concentration of binding sites).

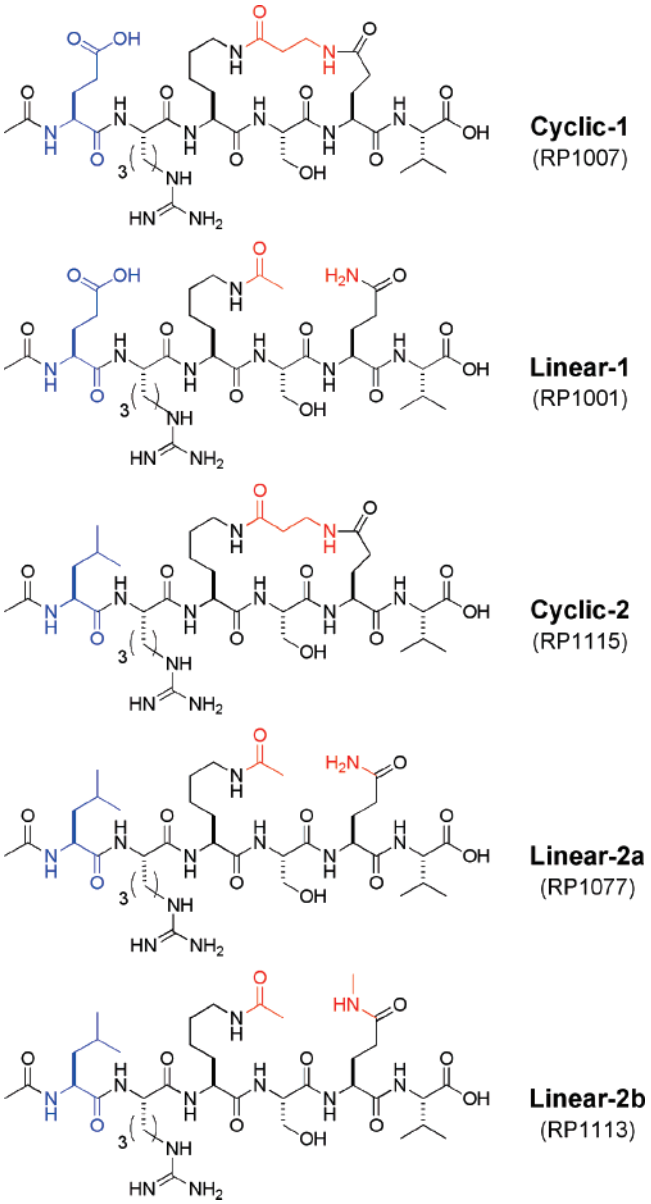

FIGURE 9: Structures of cyclic and linear control ligands for PDZ10.

of engaging in neuronal signaling events, as a component of the NMDAR signaling complex in hippocampal neurons (*4*). From a medicinal perspective, a notable association for MUPP1 is its connection to high-risk human papillomavirus (HPV), the 18 E6 protein of which is carcinogenic and is associated with the development of cervical cancer (*26*). This points to potential therapeutic relevance once the underlying biochemistry and pharmacology of MUPP1 are established, for which our ligand development and characterization is intended as a preliminary step.

At the substructural level, the binding properties of the individual MUPP1 PDZ domains are poorly understood. Although interactions involving PDZ9 (*9*, *27*) and PDZ13 (*28*) have been reported, it is PDZ10 that is to date the best characterized of all 13 domains. PDZ10 has been shown to interact with the C-terminal tails of a variety of proteins, although these are based on qualitative binding assessments (e.g., yeast two-hydrid and pulldown experiments), and not on analyses that provide equilibrium constants. These reported partner proteins include the 5-HT_{2a} and 5-HT_{2c} serotonin receptors (*2*), hTapp1 and mTapp2 (*6*), adenovirus E4ORF1 (*11*), hc-kit (*5*), claudin-1 (*9*, *10*), HPV-18 E6 (*11*), NG2 (*8*), and TARP (*7*).

Each of these protein partners is affiliated with a particular set of cellular effects, and the study reported here seeks to implement a first step toward molecular probe development, with which to advance the characterization of the role of PDZ10 in these processes. By definitively establishing the magnitude of binding for each partner protein—or, in this study, shorter peptides to serve as surrogates—one can rank order the interactions that appear to be quantitatively meaningful and winnow out those whose affinities appear insubstantial. This, of course, does not prove weaker interactions are biologically insignificant, especially since we use peptide proxies in place of the actual partner proteins, but it does provide a rational basis upon which to prioritize subsequent investigations. These will then be facilitated by preparing peptide and peptidomimetic ligands based on the data obtained here, for use in developing molecular probes for cellular studies of PDZ10-mediated events.

A Calorimetric Approach to Binding Analysis. We have previously made extensive use of ITC in a program to design and develop linear (*12*, *29*) and macrocyclic (*23*, *30*) ligands for the third PDZ domain (PDZ3) of the postsynaptic density protein PSD-95. These studies have benefited from the all-inclusive nature of ITC, a pure solution technique that provides for each of the interconnected thermodynamic binding parameters listed in eq 3, as well as the stoichiometry (n) of association and the changes in heat capacity (ΔC_p) and in protonation (Δn_{H^+}) (*31*−*33*).

$$\Delta G = RT \ln K_d = \Delta H - T\Delta S \qquad (3)$$

In this study, we apply our approach to a distinctly different PDZ domain, PDZ10 from MUPP1. In our preliminary studies with PDZ10, it was found to possess two attractive properties critical for the ensuing calorimetric studies. First, it could be expressed, processed, and purified in the large quantities required for ITC experiments, and

second, CD analysis showed that PDZ10 maintains its structural characteristics at temperatures well below and above those employed for the ITC measurements in this study.

PDZ10 Binding Enthalpy Is Not Coupled to Net Proton Transfer. Any significant enthalpic interference by protonation or deprotonation upon binding of ligands to PDZ10 was ruled out through calorimetric measurements in the presence of buffers with varying heats of ionization. Since measured ΔH values from an ITC experiment are global, determining the heat change specifically associated with the protein−peptide interaction itself requires additional analysis to elucidate $(n_{H^+})\Delta H_{ion}$ in eq 1. With three different peptides (Figure 3), we observe that the net number of the protons exchanged with solvent upon complex formation is well below unity, and represents only a 1.9−6.6% contribution to the observed ΔH. This clearly indicates that the effect of buffer ionization on the total enthalpy of association is negligible, and hence, ΔH_{bind} is assumed to approximate ΔH within experimental error. The small contribution of $(n_{H^+})\Delta H_{ion}$ may be due to the absence of, or only slight shifts in, the pK_a of one or more groups upon complex formation or, alternatively, the compensatory effects of a large number of groups.

PDZ10 Binding Does Not Continuously Improve with Length of 5HT$_{2c}$ Peptides. Given its primacy among the attributed binding proteins for PDZ10, the serotonin receptor type 2c terminal sequence was selected for the evaluation of the effect of varying ligand length (Table 1 and Figure 5). A tetrapeptide bound at modest strength, with a K_d of 57 μM. The association was dominated by a favorable change in enthalpy, which foreshadowed the binding tendencies exhibited for each of the longer 5HT$_{2c}$ peptides. Addition of one more residue to the amino terminus improved affinity 5-fold, with a K_d of 11 μM. This pentapeptide embodied the minimal size requirement wherein most of the binding strength is captured, and beyond which further extension failed to dislodge K_d values from the ~10 μM mark. A similar ebb in binding strength with an increase in peptide length was observed in the interactions of PDZ3 of PSD-95 and three series of peptides based on CRIPT, neuroligin-1, and citron (*29*). With PDZ3, the affinity increased on ligand elongation of up to 6−8 residues, thereafter leveling off.

5HT$_{2c}$ Peptides with Free Amino Termini Exhibit Improved Affinity. With two exceptions, all the peptides in this work were acetylated at the N-terminus, to mimic the backbone character of the corresponding protein partners from which they were derived. Peptide ligands with an unmodified amino terminus can possess an additional site for protonation, fostering different forms of molecular interaction. The first point is often a practical experimental consideration, since aqueous solubility of ligands is important in ITC, as they are required in high concentrations in the injecting syringe prior to titration. With regard to energetic analysis, the direct comparison of the binding behaviors of paired N-acetylated and free amino peptides aids in deciphering the contribution of the terminal amine group.

In the study with PDZ10, the binding analysis of two non-acetylated peptides based on the 5HT$_{2c}$ sequence was evaluated (Table 1). The improved affinity of the non-acetylated peptides pinpoints the terminal free amine group as a favorable contributor to ΔG. The improved affinity was a result of a favorable enthalpy change for the hexapeptide, while an increased entropic contribution was found for the decapeptide. While the former might exemplify a prediction of improving ΔH due to net formation of a discrete molecular interaction, the latter demonstrates that such rationalization can easily prove ineffectual given the unpredictable nuances accompanying protein−ligand associations.

PDZ10 Prefers 5HT$_{2c}$ Peptides with Ser over Thr at the Critical P$_{-2}$ Position. The parent 5HT$_{2c}$ peptide bearing a serine was only slightly favored, with a K_d of 8.5 μM versus that of 13 μM exhibited by the threonine analogue (Table 1). Of more significance are the changes in enthalpy and entropy; the simple addition of a single methyl group to the β-position of Ser to yield Thr results in a $\Delta\Delta H$ of 1.5 kcal/mol and a $T\Delta\Delta S$ of 1.3 kcal/mol. The entropic favorability of threonine could be rationalized as a desolvation phenomenon, whereby additional water molecule equivalents are released upon complex formation, or it is possible that the branched side chain is to some degree preorganized in a conformation suitable for binding, resulting in a reduced entropic penalty of association.

Phosphorylation of the Ligand Reduces the Level of PDZ10 Binding. Reversible phosphorylation has been proposed as a possible mechanism by which a PDZ domain-mediated interaction might be regulated (*34*), and specific phosphorylation events have been shown to inhibit PDZ domain-mediated interactions in vivo (*35*, *36*). With respect to PDZ10 and 5HT$_{2c}$, although no specific kinases are known that selectively phosphorylate the terminal serines of the 5HT$_{2c}$ receptors in vivo, mutational studies suggest a link between the PDZ domain recognition motif and endogenous phosphorylation (*37*, *38*). Deletion of the three C-terminal residues (SSV) in 5HT$_{2c}$ of fibroblasts, for example, led to the abolition of receptor phosphorylation (*38*). In the context of our peptide model system, the two 5HT$_{2c}$ peptides with phosphoserine for serine at P$_{-1}$ and P$_{-2}$ led to a substantial decrease in the affinity of the peptides for PDZ10 (Table 2). This supports the possibility that serine phosphorylation within the critical PDZ domain recognition motif could regulate the interaction of 5HT$_{2c}$ with PDZ10. In both phosphoserine peptides, the decrease in binding affinity is a direct result of a reduction in enthalpic contributions of 1.2−1.5 kcal/mol, which could be rationalized as the loss of the β-hydroxy-mediated hydrogen bonding of the native Ser residue. Furthermore, phosphorylation results in larger steric bulk that may lead to the increase in steric hindrance and perturbation of the ligand from an otherwise favorable binding mode.

PDZ10 Exhibits a Range of Binding Affinities for Partner Protein Sequences. In addition to providing insight into the factors that govern PDZ10 binding, ligands based on known or putative endogenous interaction partners may serve as starting points for the development of specific molecular probes for use in future cellular and biological investigations. The protein partners selected for study here are participants in a wide range of cellular functions. Analysis of the parameters for the nine partner-derived sequences (Table 3 and Figure 7) revealed widely variable thermodynamic outcomes for complexation to PDZ10. In terms of equilibrium binding strength, a 40-fold span separated the highest-affinity hc-kit sequence and the lowest-affinity HPV-18 E6 ligand.

The association of the hc-kit peptide showed a remarkably favorable enthalpy change of −10.5 kcal/mol, which might denote a large number of discrete binding interactions (e.g., electrostatic and hydrogen bonding) upon complex formation. Conversely, the binding entropy was very unfavorable, with a $T\Delta S$ at −3.3 kcal/mol, indicating a substantial loss of degrees of freedom upon binding. The peptides $5HT_{2c}$, mTapp2, and E6 are neutral in this regard, with nearly noncontributing entropy. Peptides $5HT_{2a}$, hTapp1, and claudin-1 make a substantial entropic contribution, while NG2 and TARP possess dominant entropic contributions.

Without further parsing the individual thermodynamic parameters, we find striking the sheer range of sequences that PDZ10 is capable of recognizing. Using a binding window of only just under 10-fold, from the $5HT_{2c}$ ($K_d \sim 8$ μM) to claudin-1 ($K_d \sim 77$ μM) sequences, the P_{-1} position can accommodate Ser, Cys, Asp, Pro, Trp, and Tyr. While P_{-2} retains a strong preference for the conserved Thr or Ser of a class I PDZ domain, Tyr and Asp can also substitute, if somewhat less reliably. When structural characterization becomes available for PDZ10 in complex with peptides, it will be interesting to see how the protein manages to accommodate such side chain diversity and whether significantly different binding modes will be observed.

A review of the data from all of the protein partner peptides prompts the question of how the PDZ domain binding behavior of these peptides would compare with that of the *whole* partner proteins from which they are derived. Since such PDZ10−protein interactions have not yet been assessed, this is currently just a matter of conjecture. It can be reasoned that the C-terminal region of the partner protein is in some way conformationally biased or restricted, lacking the full flexibility of their linear peptide models, and as such preorganized for association. This argument is especially important for hc-kit, $5HT_{2c}$, $5HT_{2a}$, NG2, TARP, and claudin-1 proteins, which are receptors or membrane-associated and perhaps more restricted or preorganized, and obviously locally more concentrated, than the cytosolic proteins, hTapp1, mTapp2, and HPV-18 E6. Furthermore, the C-terminus of the PDZ10 binding protein might be part of a larger molecular recognition motif, where additional residues on the surface of either the partner or PDZ10 might participate in the formation of additional molecular interactions. Even if the actual affinities of protein partners differ from their corresponding peptide models, one wonders whether these protein partners would display a parallel pattern of differential binding strengths. That is, would the preferred order for PDZ10 association (hc-kit > $5HT_{2c}$ > $5HT_{2a}$ > mTapp2 ∼ hTapp1 > TARP ∼ NG2 > claudin-1 > HPV-18 E6) as seen with the short peptides in vitro likewise be observed with the actual partner proteins in vivo? This questions the biological significance of such thermodynamic values and their ultimate role in the interactions within the cell. It is interesting to note that PDZ domains are generally believed to be part of transient complexes, many considered regulatory in nature (as seen in regulation by phosphorylation and dephosphorylation), and variability in the binding affinity with which PDZ10 interacts with endogenous partners may be a function of its cellular roles. Thus, a spectrum of binding affinity values for multiple partners might be reasonable to expect for a particular PDZ domain such as PDZ10.

Modest Binding Improvement through Consensus Sequence. A consensus octapeptide, loosely templated on the $5HT_{2c}$ peptide in which residues from other partner protein-derived sequences were substituted, yielded an affinity only slightly better than that of the parent sequence. Substitutions within that consensus sequence led to Ac-VSLRVSSV, with a K_d of 4.2 μM (Table 4); this represents an affinity 2-fold higher than that of the native $5HT_{2c}$ peptide as a result of a large improvement in entropy. Peptides $5HT_{2c}$ (Ac-VSERISSV) and Ac-VSLRVSSV are different only at positions P_{-3} (Ile vs Val) and P_{-5} (Glu vs Leu). The difference at P_{-3} is only that of an extra carbon equivalent (with Val sporting one fewer methylene group than Ile), while at P_{-5}, the acidic side chain is replaced with a hydrophobic group. While this is speculation that will require additional analogue preparation and testing, this more significant structural change at P_{-5} could be responsible for the difference in the solvation entropy (i.e., entailing release of an ordered shell of water molecules upon complex formation) between the two peptides, perhaps accounting for the favorable $T\Delta\Delta S$ of ∼1.6 kcal/mol.

Surface Character of PDZ10 Association Can Be Estimated with ΔC_p. Any molecular association in which water is released from the surface leads to a substantial change in heat capacity proportional to the amount of the surface involved (*16*). Through this correlation, ΔC_p provides a link between thermodynamic data and macromolecular structure. Currently, no structural information about PDZ10 is available, and so it is not possible to directly relate the thermodynamic binding parameters to structures of the free protein, ligands, and the resulting complexes. However, binding enthalpy and heat capacity changes at specified temperatures have been proposed to relate to changes in the polar and apolar solvent accessible surface areas, ΔASA_{polar} and ΔASA_{apolar}, respectively, upon complex formation (*39*, *40*). At 25 °C, a calculated value for the change in heat capacity can be correlated to these changes in surface accessibility (eq 4).

$$\Delta C_p = (0.45)\Delta ASA_{apolar} - (0.26)\Delta ASA_{polar} \quad (4)$$

For a bimolecular interaction involving rigid bodies, ΔH changes linearly with temperature; i.e., ΔC_p is temperature-independent (*17*). As a result, at a reference temperature of 60 °C, the enthalpy function is related to the contributions of polar and apolar surface area changes (*39*, *40*) (eq 5)

$$\Delta H_{60} = (31.4)\Delta ASA_{polar} - (8.44)\Delta ASA_{apolar} \quad (5)$$

where ΔH_{60} is the total binding enthalpy at 60 °C and can be calculated from ΔH at a specified temperature and measured ΔC_p.

Using both equations, the change in surface area values was calculated; the result is that the burial of polar and apolar surface areas contributes nearly equally to the energetics of the binding event (Table 5). The change in polar surface area arises as a result of hydrogen bonding and van der Waals interactions, while the change in apolar surface area connotes the release of water as a result of association, i.e., a hydrophobic interaction. Burial of nearly equal polar and apolar surface areas in the molecular association of PDZ10

and the studied peptides implies that the contribution from the dual effect of hydrogen bonding and van der Waals interactions is on par with the contribution from the hydrophobic interactions. The combined magnitudes of the surface area changes are significantly greater for Ac-VSLRVSSV another possible indication of the direct involvement of the P_{-5} (Leu) side chain in the interaction.

Bridged Cyclic Peptides Can Serve as Ligands for PDZ10. Linear, unmodified peptides can be quite useful for molecular recognition studies, but their utility for in vivo assays can often be compromised by their susceptibility to endogenous proteases. Cyclic peptides, however, often possess superior stability properties in a cellular environment. The cyclic peptides prepared here were based on a strategy we devised and successfully implemented during earlier work in developing conformationally constrained peptide macrocycles for the third PDZ domain (PDZ3) of neuronal PSD-95 protein (*23*, *30*). Considering that no structure of PDZ10 was available and we did not prepare or assay an assortment of variable-sized macrocycles, it was heartening to observe that the β-Ala bridging unit did yield ligands with reasonable binding affinities (Table 6 and Figure 9).

The cyclic peptides studied here were designed from the sequences of the $5HT_{2c}$ peptide (for **Cyclic-1**) and high-affinity peptide Ac-VSLRVSSV (for **Cyclic-2**), where in both cases the P_{-1} and P_{-3} residues were changed to glutamate and lysine, respectively. The side chains of these two residues were bridged by coupling β-alanine to yield two new amide bonds, which effected the cyclization.

A priori, it was recognized that the cyclic peptides might incur an energetic binding penalty due to unfavorable steric or electronic factors associated with the change in the identity of two residues, and the addition of the bridging β-Ala unit. Since PDZ10 has not been structurally characterized, this design was not bolstered by the same structure-based rationale like our earlier macrocycles prepared for PDZ3 of PSD-95. We speculated, however, that the dominance in binding of the P_0 and P_{-2} positions over the P_{-1} and P_{-3} positions might be operative in PDZ10 as we had observed with PDZ3 and therefore pursued a corresponding cyclization strategy. Further, with the intent of preparing peptides that were smaller and more likely to possess desirable stability and possible cell permeability properties, the macrocyclic backbone comprised six instead of the eight residues used in the earlier binding studies.

Cyclic-2 peptide exhibited a 3-fold higher potency than **Cyclic-1**. The sole difference between the two ligands was Glu (**Cyclic-1**) versus Leu (**Cyclic-2**) at P_{-5}, indicating the importance of that position in a presumed hydrophobic interaction. Both hexapeptide macrocycles exhibited lowered affinity values compared to those of the linear octapeptide $5HT_{2c}$ and Ac-VSLRVSSV sequences from which they were designed. The loss of binding strength was due to an unequal energetic compensation in which a large and unfavorable change in enthalpy countered a substantial and favorable increase in entropy.

To more meaningfully compare the effect of cyclization, three linear control peptides were prepared that resembled a "precyclized" version of the macrocycle. For both **Cyclic-1** and **Cyclic-2**, nearly total enthalpy−entropy compensation was observed, and in both cases, entropy is the dominant factor.

Conclusions. This investigation demonstrates that effective binding ligands for the PDZ10 domain of MUPP1 can be derived from the C-terminal regions of designated partner proteins. In a single linear series, calorimetry demonstrates that modest binding is achieved with only four residues, and that near-maximal affinity is obtained with five or six residues, beyond which further additions do not appear to make a favorable net contribution. The presence of phosphorylation at P_{-1} or P_{-2} Ser negatively impacts binding to PDZ10, which may provide evidence to support broader assertions of cellular regulation in this manner. Further, variation in sequence leads to a continuum of affinity values that spans more than 40-fold. The efficacy with which partner protein-derived peptides serve as binding ligands may provide some indication of the affinity of the native interaction with the intact protein partner, but the extent to which this will be appropriate cannot yet be validated, since binding constants for the actual protein−protein interactions mediated by PDZ10 are not available. Finally, the P_{-1}/P_{-3} bridging strategy we devised earlier to generate cyclic ligands for a different PDZ domain was successfully applied to PDZ10. Previously, we had found that a PSD-95 PDZ domain-targeting macrocycle could inhibit interactions in transfected cells, with lifetimes longer than those of linear peptides (*41*). Macrocycles such as the higher-affinity **Cyclic-2** might eventually find similar service as a molecular probe in support of cellular studies of MUPP1 PDZ10 function.

ACKNOWLEDGMENT

We thank L. Hryhorczuk (Wayne State University) for mass spectrometry services.

SUPPORTING INFORMATION AVAILABLE

Circular dichroism spectra of PDZ10 at different temperatures and data for the changes in enthalpy of three representative peptides in variable buffers and at variable temperatures. This material is available free of charge via the Internet at http://pubs.acs.org.

REFERENCES

1. Ullmer, C., Schmuck, K., Figge, A., and Lubbert, H. (1998) Cloning and characterization of MUPP1, a novel PDZ domain protein, *FEBS Lett. 424*, 63−68.
2. Becamel, C., Figge, A., Poliak, S., Dumuis, A., Peles, E., Bockaert, J., Lubbert, H., and Ullmer, C. (2001) Interaction of serotonin 5-hydroxytryptamine type 2C receptors with PDZ10 of the multi-PDZ domain protein MUPP1, *J. Biol. Chem. 276*, 12974−12982.
3. Heydecke, D., Meyer, D., Ackermann, F., Wilhelm, B., Gudermann, T., and Boekhoff, I. (2006) The multi PDZ domain protein MUPP1 as a putative scaffolding protein for organizing signaling complexes in the acrosome of mammalian spermatozoa, *J. Androl. 27*, 390−404.
4. Krapivinsky, G., Medina, I., Krapivinsky, L., Gapon, S., and Clapham, D. E. (2004) SynGAP-MUPP1-CaMKII synaptic complexes regulate p38 MAP kinase activity and NMDA receptor-dependent synaptic AMPA receptor potentiation, *Neuron 43*, 563−574.
5. Mancini, A., Koch, A., Stefan, M., Niemann, H., and Tamura, T. (2000) The direct association of the multiple PDZ domain containing proteins (MUPP-1) with the human c-Kit C-terminus is regulated by tyrosine kinase activity, *FEBS Lett. 482*, 54−58.
6. Kimber, W. A., Trinkle-Mulcahy, L., Cheung, P. C., Deak, M., Marsden, L. J., Kieloch, A., Watt, S., Javier, R. T., Gray, A., Downes, C. P., Lucocq, J. M., and Alessi, D. R. (2002) Evidence that the tandem-pleckstrin-homology-domain-containing protein

TAPP1 interacts with Ptd(3,4)P2 and the multi-PDZ-domain-containing protein MUPP1 in vivo, *Biochem. J. 361*, 525−536.
7. Dakoji, S., Tomita, S., Karimzadegan, S., Nicoll, R. A., and Bredt, D. S. (2003) Interaction of transmembrane AMPA receptor regulatory proteins with multiple membrane associated guanylate kinases, *Neuropharmacology 45*, 849−856.
8. Barritt, D. S., Pearn, M. T., Zisch, A. H., Lee, S. S., Javier, R. T., Pasquale, E. B., and Stallcup, W. B. (2000) The multi-PDZ domain protein MUPP1 is a cytoplasmic ligand for the membrane-spanning proteoglycan NG2, *J. Cell. Biochem. 79*, 213−224.
9. Hamazaki, Y., Itoh, M., Sasaki, H., Furuse, M., and Tsukita, S. (2002) Multi-PDZ domain protein 1 (MUPP1) is concentrated at tight junctions through its possible interaction with claudin-1 and junctional adhesion molecule, *J. Biol. Chem. 277*, 455−461.
10. Poliak, S., Matlis, S., Ullmer, C., Scherer, S. S., and Peles, E. (2002) Distinct claudins and associated PDZ proteins form different autotypic tight junctions in myelinating Schwann cells, *J. Cell Biol. 159*, 361−372.
11. Lee, S. S., Glaunsinger, B., Mantovani, F., Banks, L., and Javier, R. T. (2000) Multi-PDZ domain protein MUPP1 is a cellular target for both adenovirus E4-ORF1 and high-risk papillomavirus type 18 E6 oncoproteins, *J. Virol. 74*, 9680−9693.
12. Saro, D., Klosi, E., Paredes, A., and Spaller, M. R. (2004) Thermodynamic analysis of a hydrophobic binding site: Probing the PDZ domain with nonproteinogenic peptide ligands, *Org. Lett. 6*, 3429−3432.
13. Wiseman, T., Williston, S., Brandts, J. F., and Lin, L. N. (1989) Rapid measurement of binding constants and heats of binding using a new titration calorimeter, *Anal. Biochem. 179*, 131−137.
14. Zhang, Y. L., and Zhang, Z. Y. (1998) Low-affinity binding determined by titration calorimetry using a high-affinity coupling ligand: A thermodynamic study of ligand binding to protein tyrosine phosphatase 1B, *Anal. Biochem. 261*, 139−148.
15. Sturtevant, J. M. (1977) Heat capacity and entropy changes in processes involving proteins, *Proc. Natl. Acad. Sci. U.S.A. 74*, 2236−2240.
16. Gomez, J., Hilser, V. J., Xie, D., and Freire, E. (1995) The heat capacity of proteins, *Proteins 22*, 404−412.
17. O'Brien, R., Ladbury, J. E., and Chowdry, B. Z. (2001) Isothermal titration calorimetry of biomolecules, in *Protein-Ligand Interactions: Hydrodynamics and Calorimetry* (Harding, S. E., and Chowdry, B. Z., Eds.) Oxford University Press, New York.
18. Spolar, R. S., and Record, M. T., Jr. (1994) Coupling of local folding to site-specific binding of proteins to DNA, *Science 263*, 777−784.
19. Mandiyan, V., O'Brien, R., Zhou, M., Margolis, B., Lemmon, M. A., Sturtevant, J. M., and Schlessinger, J. (1996) Thermodynamic studies of SHC phosphotyrosine interaction domain recognition of the NPXpY motif, *J. Biol. Chem. 271*, 4770−4775.
20. McNemar, C., Snow, M. E., Windsor, W. T., Prongay, A., Mui, P., Zhang, R., Durkin, J., Le, H. V., and Weber, P. C. (1997) Thermodynamic and structural analysis of phosphotyrosine polypeptide binding to Grb2-SH2, *Biochemistry 36*, 10006−10014.
21. Bradshaw, J. M., and Waksman, G. (1999) Calorimetric examination of high-affinity Src SH2 domain-tyrosyl phosphopeptide binding: Dissection of the phosphopeptide sequence specificity and coupling energetics, *Biochemistry 38*, 5147−5154.
22. Panse, V. G., Swaminathan, C. P., Surolia, A., and Varadarajan, R. (2000) Thermodynamics of substrate binding to the chaperone SecB, *Biochemistry 39*, 2420−2427.
23. Li, T., Saro, D., and Spaller, M. R. (2004) Thermodynamic profiling of conformationally constrained cyclic ligands for the PDZ domain, *Bioorg. Med. Chem. Lett. 14*, 1385−1388.
24. Sheng, M., and Sala, C. (2001) PDZ domains and the organization of supramolecular complexes, *Annu. Rev. Neurosci. 24*, 1−29.
25. Harris, B. Z., and Lim, W. A. (2001) Mechanism and role of PDZ domains in signaling complex assembly, *J. Cell Sci. 114*, 3219−3231.
26. zur Hausen, H. (1996) Papillomavirus infections: A major cause of human cancers, *Biochim. Biophys. Acta 1288*, F55−F78.
27. Jeansonne, B., Lu, Q., Goodenough, D. A., and Chen, Y. H. (2003) Claudin-8 interacts with multi-PDZ domain protein 1 (MUPP1) and reduces paracellular conductance in epithelial cells, *Cell. Mol. Biol. (Paris, Fr., Print) 49*, 13−21.
28. Coyne, C. B., Voelker, T., Pichla, S. L., and Bergelson, J. M. (2004) The coxsackievirus and adenovirus receptor interacts with the multi-PDZ domain protein-1 (MUPP-1) within the tight junction, *J. Biol. Chem. 279*, 48079−48084.
29. Saro, D., Li, T., Rupasinghe, C., Paredes, A., Caspers, N., and Spaller, M. R. (2007) A thermodynamic ligand binding study of the third PDZ domain (PDZ3) from the mammalian neuronal protein PSD-95, *Biochemistry 46*, 6340−6352.
30. Udugamasooriya, G., Saro, D., and Spaller, M. R. (2005) Bridged peptide macrocycles as ligands for PDZ domain proteins, *Org. Lett. 7*, 1203−1206.
31. Ward, W. H., and Holdgate, G. A. (2001) Isothermal titration calorimetry in drug discovery, *Prog. Med. Chem. 38*, 309−376.
32. Leavitt, S., and Freire, E. (2001) Direct measurement of protein binding energetics by isothermal titration calorimetry, *Curr. Opin. Struct. Biol. 11*, 560−566.
33. Jelesarov, I., and Bosshard, H. R. (1999) Isothermal titration calorimetry and differential scanning calorimetry as complementary tools to investigate the energetics of biomolecular recognition, *J. Mol. Recognit. 12*, 3−18.
34. Jelen, F., Oleksy, A., Smietana, K., and Otlewski, J. (2003) PDZ domains: Common players in the cell signaling, *Acta Biochim. Pol. 50*, 985−1017.
35. Cao, T. T., Deacon, H. W., Reczek, D., Bretscher, A., and von Zastrow, M. (1999) A kinase-regulated PDZ-domain interaction controls endocytic sorting of the β2-adrenergic receptor, *Nature 401*, 286−290.
36. Cohen, N. A., Brenman, J. E., Snyder, S. H., and Bredt, D. S. (1996) Binding of the inward rectifier K^+ channel Kir 2.3 to PSD-95 is regulated by protein kinase A phosphorylation, *Neuron 17*, 759−767.
37. Parker, L. L., Backstrom, J. R., Sanders-Bush, E., and Shieh, B. H. (2003) Agonist-induced phosphorylation of the serotonin 5-HT2C receptor regulates its interaction with multiple PDZ protein 1, *J. Biol. Chem. 278*, 21576−21583.
38. Backstrom, J. R., Price, R. D., Reasoner, D. T., and Sanders-Bush, E. (2000) Deletion of the Serotonin 5-HT2C Receptor PDZ Recognition Motif Prevents Receptor Phosphorylation and Delays Resensitization of Receptor Responses, *J. Biol. Chem. 275*, 23620−23626.
39. Murphy, K. P., and Freire, E. (1992) Thermodynamics of structural stability and cooperative folding behavior in proteins, *Adv. Protein Chem. 43*, 313−361.
40. Xie, D., and Freire, E. (1994) Molecular basis of cooperativity in protein folding. V. Thermodynamic and structural conditions for the stabilization of compact denatured states, *Proteins 19*, 291−301.
41. Piserchio, A., Salinas, G. D., Li, T., Marshall, J., Spaller, M. R., and Mierke, D. F. (2004) Targeting specific PDZ domains of PSD-95: Structural basis for enhanced affinity and enzymatic stability of a cyclic peptide, *Chem. Biol. 11*, 469−473.

BI7008135